iScience

CellPress
OPEN ACCESS

Article

Impedimetric antimicrobial peptide biosensor for the detection of human immunodeficiency virus envelope protein gp120

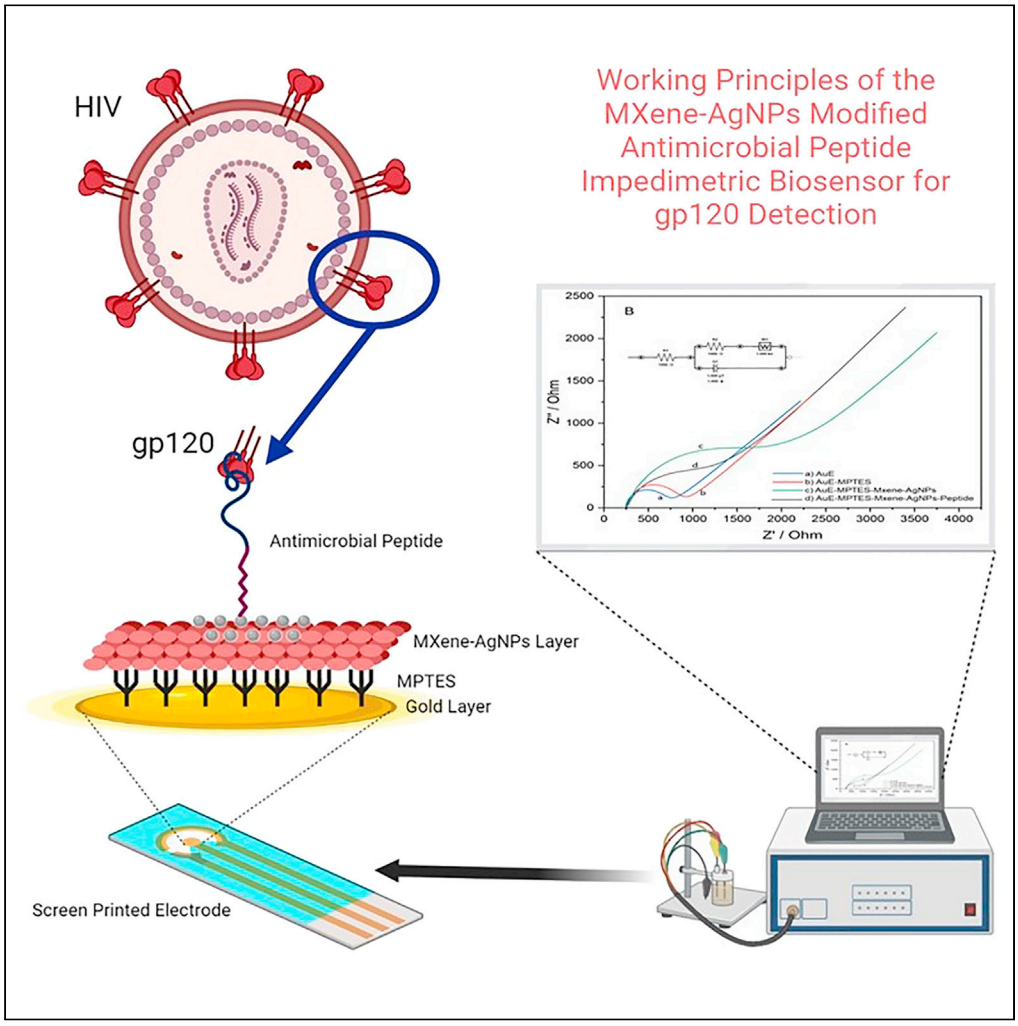

Zihni Onur Uygun, Savas Tasoglu

stasoglu@ku.edu.tr

Highlights

First impedimetric antimicrobial peptide biosensor for the detection of HIV-gp120

Detection time optimization provided by Chronoimpedance

Electrochemical label-free HIV-gp120 protein detection

Uygun & Tasoglu, iScience 27, 109190
March 15, 2024
https://doi.org/10.1016/j.isci.2024.109190

iScience

CellPress
OPEN ACCESS

Article

Impedimetric antimicrobial peptide biosensor for the detection of human immunodeficiency virus envelope protein gp120

Zihni Onur Uygun[1,2] and Savas Tasoglu[2,3,4,5,6,*]

SUMMARY

This study presents the design and implementation of an antimicrobial peptide-based electrochemical impedance spectroscopy (EIS) based biosensor system. The biosensor consists of a gold coated carbon electrode with MXene and silver nanoparticles (AgNPs) for the label-free detection of the human immunodeficiency virus (HIV) envelope protein gp120. Scanning electron microscopy was used to confirm the presence and distribution of MXene and AgNPs on the biosensor surface. The employment of the antimicrobial peptide on the electrode surface minimized the denaturation of the biorecognition receptor to ensure reliable and stable performance. The biosensor exhibited a linear range of 10–4000 pg mL-1 for gp120 detection, demonstrating good repeatability in real samples. The limit of detection (LOD) and limit of quantification (LOQ) were also calculated as 0.05 pg mL^{-1} and 0.14 pg mL^{-1}, respectively. This biosensing platform has promising applications in the detection of HIV in clinical and point-of-care settings.

INTRODUCTION

Viruses that spread rapidly can negatively affect human life across the world.[1] Taking the necessary precautions in a timely manner is required and relies on the accurate detection of virus particles. A broad range of virus species have been identified.[2] HIV infects 37 million people worldwide and leads to 1 million mortalities annually.[3] Although advances in antiretroviral therapy have been effective in reducing the spread and severity of HIV, there is not yet a definitive cure for the disease, hence patients must continue treatment throughout their lives. For an effective treatment process, it is important to constantly monitor patients for HIV viral load. Several diagnostic devices based on physicochemical receptors have been developed to detect HIV in recent years. However, they are affected by the sample composition due to the immunoassay or analysis of genetic materials. There are currently five generation test types. First-generation HIV antibody tests were diagnostic assays developed following its initial isolation in 1983.[4] These tests used enzyme-linked immunosorbent analysis (ELISA) and chemiluminescence, and proteins isolated from virus-infected tissue cultures as antigenic targets. However, since this method only detected IgG antibodies against HIV-1, false positive results were detected. In the second-generation HIV tests developed in the late 1980s, the specificity of screening procedures was increased and the positive predictive value was improved by adding recombinant antigens, particularly HIV-1 p24, to the antigen medium. These second-generation assays reduced the antibody negative state to 4–6 weeks post infection. These tests could detect HIV-2 antibodies in addition to HIV-1 antibodies.[5] The addition of IgM detection to the test procedure resulted in third generation HIV testing. The fourth generation HIV tests combined antibody and antigen detection, using ELISA and chemiluminescence techniques. The test reduced the negative state to 2 weeks. While both antibodies and antigens were detected in these procedures, these tests only produced a single result, but it cannot be distinguished whether a positive result is due to the presence of HIV-1 p24 antigen or antibodies to HIV-1.[6] Fifth generation tests began after the FDA approved the Bio-Rad BioPlex 2200 HIV Ag/Ab screening test which used a multiplex analysis method as a diagnostic test in 2015. Similar to the fourth-generation procedures, this test detected both HIV antibody and HIV-1 p24 antigen, but provided results separately for each analyte. These were able to detect Ig and proteins; therefore, false positive signals were produced. Thus, more accurate, repeatable, sensitive, and even reusable tests are desired to reduce costs.

A biosensor is composed of a biological recognition receptor[7] and a physicochemical transducer.[8] The biorecognition receptor interacts with an analyte and forms a physicochemical signal that is sensed and transferred to an analyzer using a transducer. The challenging aspect of a biosensor system is the biorecognition element, which can be affected by environmental conditions or sample characteristics such as temperature, pH, and ionic strength, leading to conformational changes and preventing analyte interaction. Furthermore, denaturation and the low regeneration potential of the biorecognition receptors are limitations of biosensor systems.

[1]Kafkas University, Faculty of Medicine, Department of Medical Biochemistry, Kars 36100, Türkiye
[2]Koç University, Koç University Translational Medicine Research Center (KUTTAM), Istanbul 34450, Türkiye
[3]Koç University Arçelik Research Center for Creative Industries (KUAR), Koç University, Istanbul 34450, Türkiye
[4]Koç University, Engineering Faculty, Department of Mechanical Engineering, Istanbul 34450, Türkiye
[5]Boğaziçi University, Boğaziçi Institute of Biomedical Engineering, Istanbul 34684, Türkiye
[6]Lead contact
*Correspondence: stasoglu@ku.edu.tr
https://doi.org/10.1016/j.isci.2024.109190

In this study, a biosensor is engineered using antimicrobial peptides without denaturation. To detect HIV, an envelope protein was chosen. HIV envgen encodes the only surface-expressed viral protein Env, a 160 kD (gp160) glycoprotein required for attachment and entry into host cells. After translation, gp160 is cleaved into gp120 and gp41, which remain non-covalently linked to form a single subunit of a trimeric "spike" on the virion surface.[9] The C-terminal subunit, gp41, contains a cytoplasmic domain (subsequently inside the viral membrane), a membrane spanning domain, and an extracellular domain that mediates the conformational change required for fusion.[10,11] The N-terminal subunit, gp120, is completely outside the viral membrane and this protein is used as an important biomarker in HIV diagnosis. The host receptor CD4 initiates infection by interacting with gp120.[12] To prevent denaturation by detecting this biomarker, the Database of Antimicrobial Activity and Structure of Peptides (dbaasp.org) revealed an antimicrobial peptide with a high affinity for gp120.[13] To increase the surface stability, conductivity, and area, we used MXene with AgNP modifications that provide the immobilization of antimicrobial peptides through silver to MXene.[14] MXenes are layered nanomaterials with a large surface area, which is useful for biosensor technology, as these are often used in order to immobilize more biorecognition receptors and increase the sensitivity of the biosensor. Owing to their electronic properties, MXenes have been used mostly with oxidizing agents to develop oxidation/reduction type biosensors.[15,16] The composite can reduce the target molecule such as a peroxide, like a mediator, and amplify the signals. Moreover, these materials (MXenes) can either be used as adsorption-based modification materials or covalent biomolecule immobilization nanomaterials.[15–18] Therefore, these versatile properties and advantages lead us to choose MXene as an immobilization agent. However, we needed to modify MXene using a particle, which would be able to form self-assemble bonds. We chose to apply silver nanoparticles on the MXene layers since sliver nanoparticles could directly be reduced and synthesized by using the inherent reduction capability of MXene. This modification was chosen because the one bench synthesis of the MXene-AgNPs provided the same nanocomposite usage for the entire study, which increased repeatability by using the same bench material. This strategy also allowed for the simple modification of MXene with silver in generating the immobilization material. Its conductivity, surface area, and the nanocomposite properties were leveraged for biosensor immobilization.[19] In conclusion a label-free detection technology was developed using electrochemical impedance spectroscopy (EIS) of HIV envelope protein gp120 with an antimicrobial peptide biosensor, which was modified by MXene-AgNPs.

RESULTS

An antimicrobial peptide modified biosensor was developed on a MXene-AgNP modified electrode by covalent modifications. A gold layer on carbon substrate was used for further modifications. The gold deposition process was chosen because gold clusters increase the surface area more than current commercialized screen-printed gold electrodes as verified by SEM images. Screen printed gold electrodes, on the contrary to our gold deposited electrode, have a planar gold surface. However, our electrode has spherical clusters to increase the surface area of binding MPTES. MPTES was used to facilitate easy binding to gold electrodes via SH bonds. According to the Au-SH bond and the covalent binding of MXene layers on gold electrode, 3-mercaptopropyltrimethoxysilane was used to modify gold electrodes via Au-SH bonds and silane groups formed bonds via OH groups to MXene layers. SH end group peptides were immobilized on MXene-AgNPs layers via Ag-SH bonds. Silver nanoparticles have the ability to bind SH groups.[20] This characteristic is considered a novelty for peptide immobilization via SH bonds as self-assembly monolayers. The other advantage is that AgNPs can be electrochemically oxidized at −0.8 V which proved very useful for our study, because we used 180mV potentials for impedimetric measurement. Therefore, the surface had no effect on electrochemical detection. MXenes are two-dimensional transition metal carbides[21,22] and include layers to increase the surface area as nanomaterial. Therefore, we can immobilize more biorecognition receptors to increase sensitivity. In order to lower the adsorption of the redox probe to the surface, negative charges were used to repel the negatively charged redox probe adsorption. Moreover, this strategy was employed to increase the positively charged peptides. Figures 1 and 2 shows the modification steps. Figures 1A and 1B shows the electrochemical investigation of the biosensor modifications, which were carried out by a redox probe. The oxidation and reduction signals of the redox probe provided the electrochemical investigation of the surface. Figure 1A illustrates the electrochemical modification layers of the biosensor by CV. Gold layer had high conductivity, as shown by the red colored curve. Afterward, silane modifications provided OH groups on the electrode surface that repelled negatively charged redox probes and decreased the peak current as a black color CV. Surface modified MXenes and AgNPs provided more surface area and conductivity, however F and OH groups on MXene provided more negative charges that repelled the negatively charged redox probe. This electrostatic migration reduced the concentration of the redox probe on the surface and decreased the CV peak current (shown in green). Finally, the modification of the peptide on the surface increased the peak current because of the positively charged antimicrobial peptides as blue CV. In Figure 1B, the impedance curves provided correlation with CV data. In contrast to the CV current peaks, EIS resulted in changes of electron transfer resistance on the surface. This degree of change was observed because the MXene layers have OH and F groups, which provided highly negative charges. Those negative charges repel the redox probe from the surface. Besides the conductivity, the surface acted like a negatively charged redox probe repellant. In EIS, we examined an electron, which was formed by the redox reaction of the probe, by applying 180 mV DC and frequency-based current by applying 10 mV AC to detect the electron movement through the surface, which is termed electron transfer resistance (Ret). This resistance is the reverse of the CV results (Figure 1B). The redox probes were repelled and the diffusion was controlled. Figures 2A–2D represents the SEM with EDX images with elemental analysis of the surface. Figure 2A shows the gold coated carbon electrode, elemental analysis shows the localized Au and C (Figure 2A). Figure 2B shows the MPTES modification, which included Si and S atoms (Figure 2B). Figure 2C shows the modification of the MXene layer modified with AgNPs, and D shows the MXene-AgNPs and peptide modifications, respectively. To illustrate the entire modification, Figure 2C shows a small number of MXene-AgNPs modifications, that does not reflect the final AMP immobilization process. Moreover, the proof of the MXene immobilization and the gold layer below it was demonstrated. Figure 2D shows the full cover of the surface and elemental analysis. Figure 2D shows

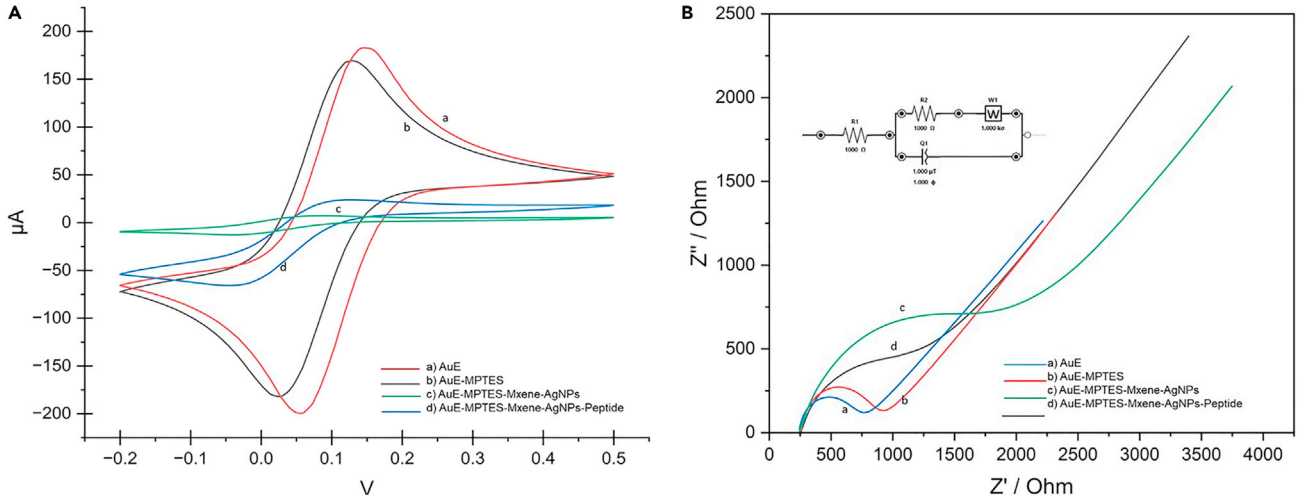

Figure 1. Electrochemical analysis of the modification of the HIV envelope gp120 protein biosensor surfaces

(A) CV analysis.

(B) EIS analysis.

no gold or silane on the surface because it is fully covered by MXene-AgNPs. The presence of S and N atoms proved that peptides were immobilized on the surface. After the biosensor modification processes, the biosensor response for the gp120 protein and the real sample matrix effect was tested chronoimpedimetrically (Figure 3). This non-faradic method measured the electrode surface resistance in time with frequency-based potentials. This frequency was chosen as 580 Hz by the Bode plot of the peptide modification step. The reaction was carried out in Pi buffer, serum sample, and gp120 spiked serum samples. Pi buffer had no increase on impedance (Figure 3 green line). The black line represents the serum samples. After 15 min, there was a constant increase without showing saturation that represented the adsorption to the surface. The red line represents the gp120 spiked serum sample. A dramatic increase was recorded at the initial point and subsequently increased (red line). After 15 min, the increases continued but the serum sample without spike also increased. Therefore, the detection time of gp120 was chosen as 15 min of incubation. This data also showed the selectivity of the biosensor. The biosensor showed adsorption instead of cross-reactivity. Two biosensors were prepared by AuE-MPTES-MXene and AuE-MPTES-AgNPs. Two electrodes were tested with the same concentration of AMP and 50 pg mL^{-1} of gp120 proteins. Au-MPTES-MXene showed no response because AMP immobilization was not successful that can be seen in CV EIS results (Figures S1A and S1B MXene modified gp120 biosensor (A: modifications by CV, B: Modifications by EIS). There was no increase after AMP immobilization and gp120 detection. The second biosensor showed a slight increase with AMP immobilization. However, it did not show any increase at a concentration of 50 pg mL^{-1}. Only MXene modification has no SH binding site, therefore AMP immobilization did not occur. Only AgNPs modification on the silane layer formed with adsorption and the washing the removal of the unbounded process, possible all were washed away and there were no signal changes. The AgNPs process was also confirmed that the gold layer was fully covered, where no AMP binding to the surface was observed. There are slight changes in EIS and CV however, this biosensor was not as sensitive as that with MXene-AgNPs modifications (Figures S2A and S2B AgNPs modified gp120 biosensor (A: modifications by CV, B: Modifications by EIS)). Afterward, the biosensor was tested for calibration curve with EIS (Figure 4A). Standard gp120 samples were incubated repeatedly from the concentrations of 10–4000 pg mL^{-1}. Concentration versus EIS data was calculated to reveal the characteristic EIS curve form (Figure 1B). The circuit model of EIS calculation was constructed by the EIS curves (Figure 1B). With the reference of these EIS curves, the elemental circuit model includes R_1 as solution resistance between the counter and working electrode; R_2, or Ret, represents the biosensor surface transfer resistance; W is the Warburg impedance that shows the mass transfer of the redox probe to the surface; and Q is the constant phase element that represents the double layer capacitive current. Instead of a capacitance element, a constant phase element was used because of the non-homogeneous surface of the biosensor. According to this circuit mode, EIS values were calculated as ohm and plotted with concentration values (Figure 4B). The calibration curve equation was also obtained y (Ret/ohm) = 4.662x (gp120 pg mL^{-1}) + 3016. This calibration curve was constructed five times, and the regression coefficient (R^2) was also calculated with its standard deviation as 0.9977 $\pm$ 0.0021. The regression coefficient showed that linearity was considered to be good and the reproducibility was higher than 99%. The reproducibility and repeatability were high because of the MXene-AgNPs nanocomposite was synthesized and used for the study, which protected its structure and the non-denaturation properties of the biorecognition elements increased the repeatable signals when regenerated. LOD and LOQ were also calculated as 0.05 pg mL^{-1} and 0.14 pg mL^{-1}, respectively. Wide calibration curve and lower limits were provided by the small size of the biorecognition element on the surface. Sy.x (Standard deviation of the residuals) was also calculated as 347.4, which was a good fit. It showed the lowest value that turned R^2 to negative value (1-Sy.x/Sy.x) calculated as −0.9971, which was close to the regression coefficient. After the calibration, the reusability of the biosensor was evaluated. Positively charged peptides were regenerated by submerging the electrode in phosphate buffer (pH 5.0). This regeneration was followed by chronoimpedance (Figure 5A). The

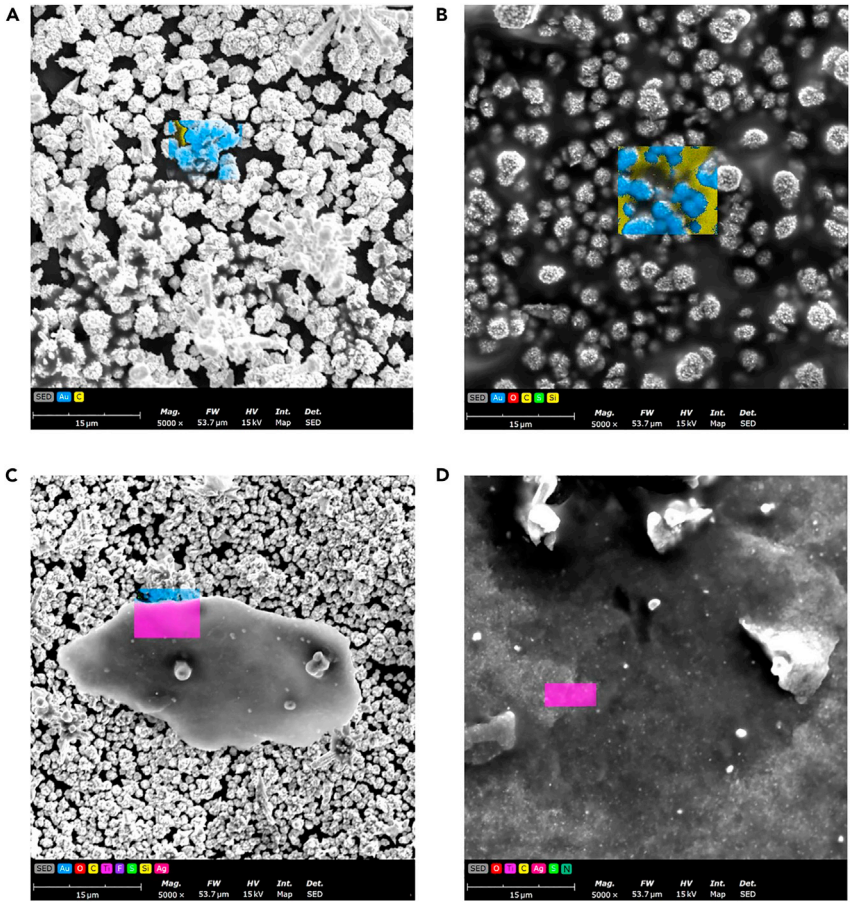

Figure 2. Scanning electron microscope with EDX analysis of the biosensor

(A) gold modified electrode.

(B) gold and MPTES modified electrode.

(C) MXene-AgNPs modified MPTES-gold surface.

(D) biosensor surface and elemental analysis.).

regeneration was 3 h. In Figure 5A, the decrease was proportional to the impedance that obtained binding time detection. Then the electrode was tested for repeating binding-rebinding cycle until it lost 10% of the first performance signal and the sensor was used 8 times for the detection of the gp120 (Figure 5B). Another optimization of real sample detection was achieved and ELISA results were compared to the biosensor. Prior to the randomly spiking process, a meaningful sample size was calculated by G-Power 3.1 program. The results were obtained using the following parameters: effected size was 0.5, alpha value was 0.05 that showed difference between two dependent means. The sample size was calculated as 45 (actual power of 0.9512). 45 samples were spiked with gp120 between 10 and 4000 pg mL^{-1} and measured by ELISA and compared to biosensor with regression analysis. The biosensor showed a good correlation with ELISA results, which were considered as gold standard, and the biosensor response between 10 and 800 showed 0.9986 and 1000–4000 showed 0.9982 regression coefficients. The slopes of the regression curves were 1.065 and 1.044, respectively. The recovery for the median gp120 protein[23] at 800 pg mL^{-1} recovery was 109% (Figure 6). The results obtained using the biosensor demonstrated higher concentrations than those of ELISA because of the positively charged peptides attracted to the negative compounds in the serum. Although the detection range of gp120 was higher than spiked samples, the repeatability deviation was lower than 16% (10 pg mL^{-1}, n = 3). The storage stability of the biosensor was also tested. Six different biosensors were constructed and three of them were stored at room temperature and the rest were stored at +4°C. No significant decrease was observed for stored samples in the fridge compared to those at room temperature (Figure 7A). Biosensors stored at room temperature were evaluated after 60 days with SEM, and a signal decrease resulted in the cracks and pinholes on the biosensor (Figure 7B). Moreover, the antimicrobial peptide nature also may provide any bacterial contamination because SEM results did not produce any significant findings. The redox probe moved these cracks to the electrode surface that changed the electrode characteristics: the semi-circle of impedance turned into two semi-circles, which meant that the redox probe reached directly under the immobilization layer. Table 1 (Table 1) shows the comparison of the biosensors that measures gp120 protein as an HIV biomarker. As demonstrated, our sensor is more sensitive and also shows superior reusability compared to other biosensors. The linear range is also quite good when compared to the ELISA method which suggests that

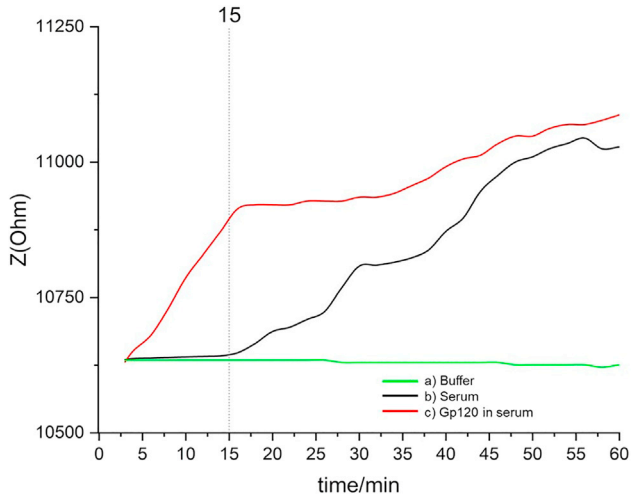

Figure 3. Chronoimpedimetric detection of gp120, green line is blank, black line is serum and red line is gp120 included serum

our biosensor is superior because of the use of nanomaterials and antimicrobial peptides which have provided more biorecognition receptor immobilizations.

DISCUSSION

HIV detection before the immunoglobulin production is challenging. The development of an antimicrobial peptide (AMP) modified biosensor on a MXene-AgNPs modified electrode presents a significant advancement in the biosensor technology, particularly using a nondenatured biorecognition receptor for the detection of HIV/AIDS detection. The comprehensive modification process involving covalent modifications, gold layer deposition, and the utilization of MXenes, AgNPs, and silane groups is noteworthy for its ability to enhance stability, sensitivity, and selectivity. The choice of gold deposition for further modifications is justified by the increased surface area provided by gold clusters, as confirmed by SEM images. This modification strategy transforms the biosensor's surface from planar (as seen in screen-printed gold electrodes) to one with spherical clusters, thereby increasing the surface area for binding MPTES (3-mercaptopropyltrimethoxysilane), which provides multiple binding sides that leads to increase sensitivity. The use of MXenes, two-dimensional transition metal carbides, further augments surface area, allowing for the immobilization of more biorecognition receptors and, consequently, increasing sensitivity. One key

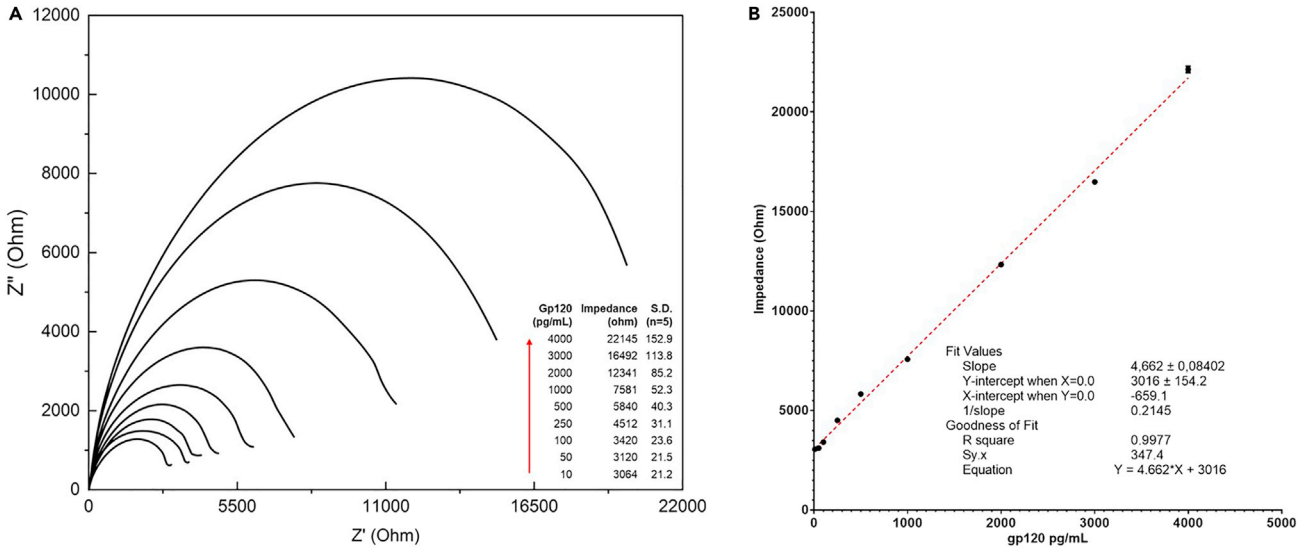

Figure 4. Calibration curve of the gp120 biosensor

(A) calibration curve with EIS.

(B) calibration curve of gp120 biosensor EIS versus concentration) y = 4.662x+3016, R^2 = 0.9977.

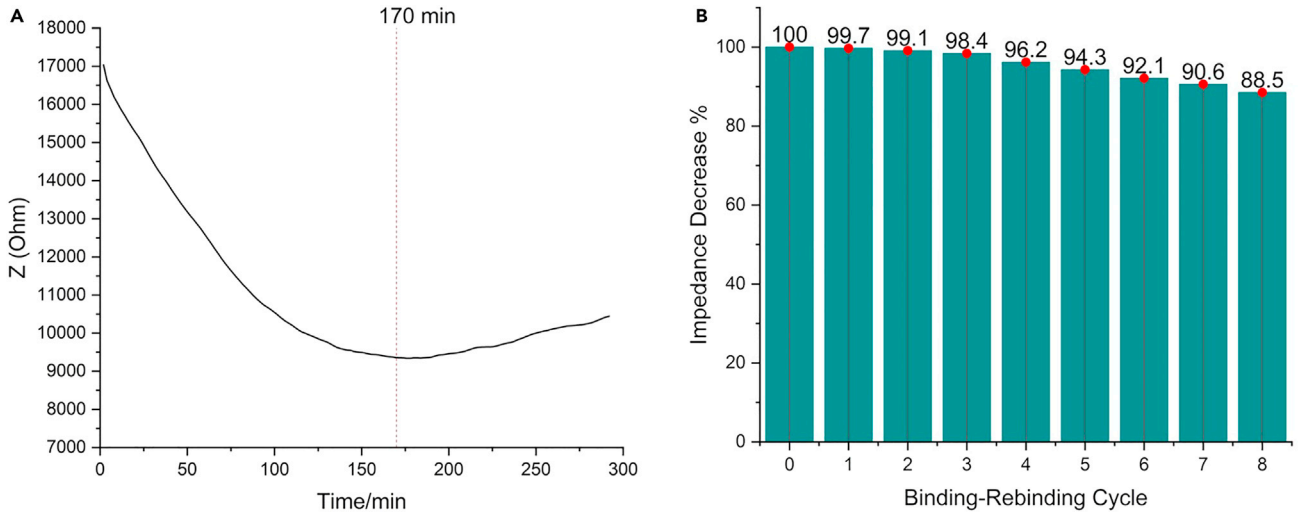

Figure 5. Investigation of the regeneration potential of the biosensor

(A) Chronoimpedimetric observation of the biosensor regeneration time in 300 min.

(B) Regeneration-rebinding cycle that shows signal loss).

innovation is the employment of AgNPs for immobilizing AMPs via Ag-SH bonds, allowing for self-assembly monolayers. The electrochemical oxidation ability of AgNPs at −0.8 V proves advantageous for impedimetric measurements conducted at +180 mV potentials. This ensures that the surface properties do not interfere with electrochemical detection, and the specific characteristics of AgNPs contribute to the success of the peptide immobilization process. The SEM images with elemental analysis validate the stepwise modification process, from gold coating to the final immobilization of peptides. The absence of gold and silane in the fully covered MXene-AgNPs layer in the final image indicates the successful immobilization of peptides on the surface. The chronoimpedimetric evaluation of the biosensor's response to gp120 protein and the real sample matrix demonstrates its selectivity, as evidenced by a distinct response to the spiked serum samples compared to the control serum and Pi buffer. The calibration curve construction and circuit model analysis further highlight the biosensor's reliability, with a high regression coefficient (R^2) indicating good linearity and reproducibility. The biosensor's reusability, as shown by the regeneration of positively charged peptides, is a valuable feature for practical applications. The biosensor's performance is superior to counterparts lacking MXene modifications or utilizing only AgNPs modifications, underscoring the significance of the nanocomposite for sensitivity. The comparison with ELISA results establishes the biosensor's credibility, with regression coefficients indicating strong correlation. The biosensor's higher concentration readings are attributed to positively charged peptides interacting with negatively charged compounds in the serum. In conclusion, the developed MXene-AgNPs modified biosensor exhibits promising features for HIV biomarker detection,

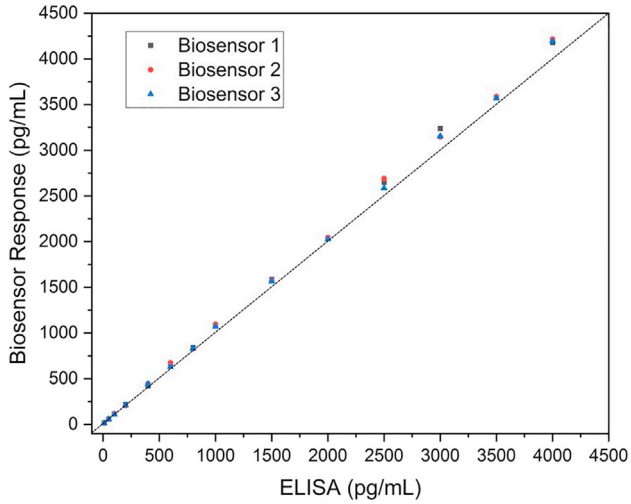

Figure 6. Comparison of the real sample analysis of the biosensor and ELISA

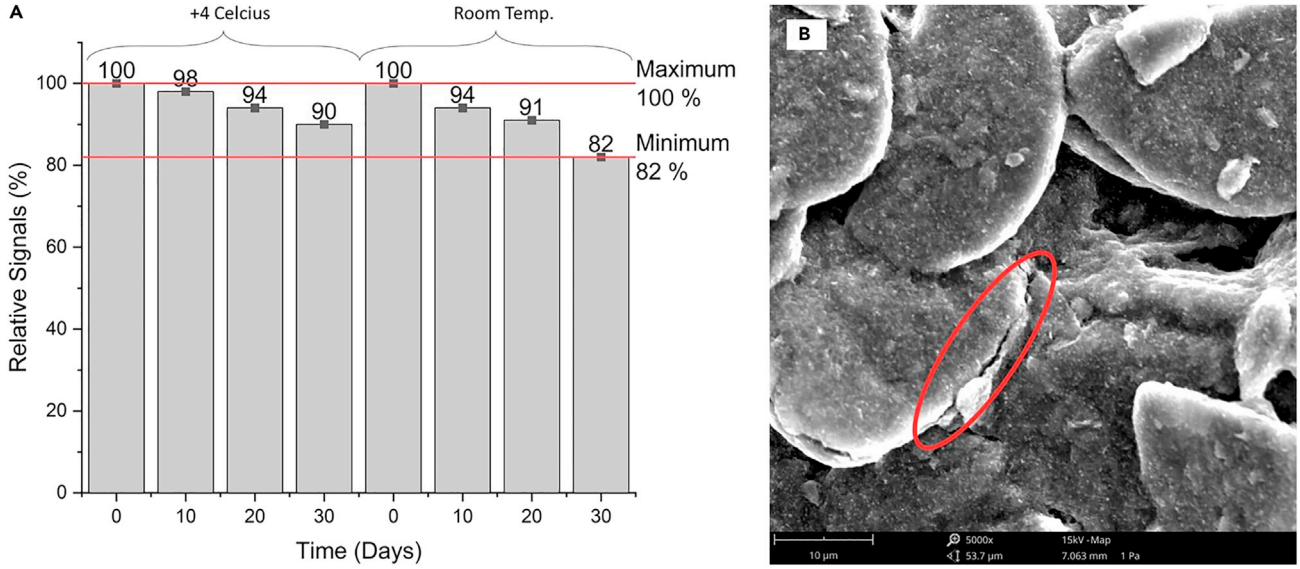

Figure 7. Storage stability of the biosensor

(A) Signal loss in time showed in bar graph until 10%.

(B) After 1-month biosensor surface change shows by SEM).

offering high sensitivity, selectivity, and reusability. The integration of nanomaterials and antimicrobial peptides represents a novel approach that outperforms existing biosensors, marking a significant step forward in biosensor technology for HIV/AIDS diagnostics.

Limitations of the study

The biosensor's storage stability, albeit better at lower temperatures, emphasizes the need for careful storage to maintain its integrity over time. Regeneration potential decreases in time. The electrode modification process is complex, which increases the costs of the study. Stability in the room temperature is problematic. In order to resolve this issue, we have ongoing experiments with different biosensors to understand the underlying mechanisms.

STAR★METHODS

Detailed methods are provided in the online version of this paper and include the following:

- KEY RESOURCES TABLE
- RESOURCE AVAILABILITY
  - Lead contact
  - Materials availability
  - Data and code availability
- EXPERIMENTAL MODEL AND STUDY PARTICIPANT DETAILS
- METHOD DETAILS
  - Chemicals and reagents
  - Electrochemical modifications and methods
  - MXene-silver nanoparticle synthesis
  - Biosensor modification and optimizations
- QUANTIFICATION AND STATISTICAL ANALYSIS

SUPPLEMENTAL INFORMATION

Supplemental information can be found online at https://doi.org/10.1016/j.isci.2024.109190.

ACKNOWLEDGMENTS

Authors acknowledge Health Institutes of Türkiye (TÜSEB) (2022-ACİL-08-11892), The Scientific and Technological Research Institution of Türkiye (TÜBİTAK) 2218 Domestic Post-Doctoral Research Program, 2232 International Fellowship for Outstanding Researchers Award (121C388 and 118C391), Alexander von Humboldt Research Fellowship for Experienced Researchers, Marie Skłodowska-Curie Individual

Table 1. Comparison of different gp120 and other HIV detecting biosensors

Biorecognition Receptor	Method	Modification	Linear Range	LOD	Reusability	Reference
Anti-gp120	Square wave voltammetry (SWV)	Au/MoS_2/Au	1 pg mL^{-1} - 10 ng mL^{-1}	0.066 pg mL^{-1}	No	Shin et al.[24]
Molecular Imprinting (MIP)	Differential pulse voltammetry (DPV)	bismuth oxides composites (CNF-Bi)	0.002–200 ng mL^{-1}	0.3 pg mL^{-1}	No	Ma et al.[25]
Anti-gp120	Cyclic Voltammetry (CV)	Au-ITO	0.6–375 pg mL^{-1}	–	No	Lee et al.[26]
Anti-gp120	ELISA	–	46.88–3000 pg mL^{-1}	11.67 pg mL^{-1}	No	SinoBiological KIT11233
Anti-gp120	ELISA	–	34.38–2200 pg mL^{-1}	14.47 pg mL^{-1}	No	Novus Biologicals NBP2-80343
Antimicrobial Peptide	Electrochemical impedance spectrocopy (EIS)	Mxene-AgNPs	10-4000 pg mL^{-1}	0.05 pg mL^{-1}	Yes	This study

Fellowship (101003361) and Royal Academy Newton-Katip Çelebi Transforming Systems Through Partnership award (120N019) for financials support of this research.

AUTHOR CONTRIBUTIONS

Conceptualization: Z.O.U. and S.T. Methodology: Z.O.U., optimization: Z.O.U. Supervision: S.T. Writing-original draft: Z.O.U., S.T. Fund acquisition: Z.O.U., S.T. Writing-review and editing: S.T.

DECLARATION OF INTERESTS

The authors declare no competing interests with respect to the authorship and/or publication of this article.

Received: September 17, 2023
Revised: October 7, 2023
Accepted: February 7, 2024
Published: February 12, 2024

REFERENCES

1. Sankaran, N., and Weiss, R.A. (2021). Viruses: Impact on Science and Society. Encyclopedia of Virology *671*, 671–680. https://doi.org/10.1016/B978-0-12-814515-9.00075-8.
2. Gelderblom, H.R. (1996). Structure and Classification of Viruses. In Medical Microbiology, 4th edition, S. Baron, ed. (Galveston (TX): University of Texas Medical Branch at Galveston). Chapter 41. https://www.ncbi.nlm.nih.gov/books/NBK8174/.
3. Soliman, M., Srikrishna, G., and Balagopal, A. (2017). Mechanisms of HIV-1 Control. Preprint at Current Medicine Group LLC *1*. https://doi.org/10.1007/s11904-017-0357-9.
4. Gallo, R.C., Sarin, P.S., Gelmann, E.P., Robert-Guroff, M., Richardson, E., Kalyanaraman, V.S., Mann, D., Sidhu, G.D., Stahl, R.E., Zolla-Pazner, S., et al. (1983). Isolation of human T-cell leukemia virus in acquired immune deficiency syndrome (AIDS). Science *220*, 865–867. 1979. https://doi.org/10.1126/science.6601823.
5. Bentsen, C., McLaughlin, L., Mitchell, E., Ferrera, C., Liska, S., Myers, R., Peel, S., Swenson, P., Gadelle, S., and Shriver, M.K. (2011). Performance evaluation of the Bio-Rad Laboratories GS HIV Combo Ag/Ab EIA, a 4th generation HIV assay for the simultaneous detection of HIV p24 antigen and antibodies to HIV-1 (groups M and O) and HIV-2 in human serum or plasma. J. Clin. Virol. *52*, S57–S61. https://doi.org/10.1016/j.jcv.2011.09.023.
6. Chavez, P., Wesolowski, L., Patel, P., Delaney, K., and Owen, S.M. (2011). Evaluation of the performance of the Abbott ARCHITECT HIV Ag/Ab Combo Assay. J. Clin. Virol. *52*, S51–S55. https://doi.org/10.1016/j.jcv.2011.09.010.
7. Uygun, Z.O. (2023). Fundamentals of biological recognition elements. Fundamentals of Sensor Technology: Principles and Novel Designs, 45–62. https://doi.org/10.1016/B978-0-323-88431-0.00017-X.
8. Turner, A.P. (1994). Biosensors. Curr. Opin. Biotechnol. *5*, 49–53. https://doi.org/10.1016/S0958-1669(05)80069-2.
9. Louten, J. (2016). Virus Transmission and Epidemiology. Essential Human Virology *71*, 71–92. https://doi.org/10.1016/B978-0-12-800947-5.00005-3.
10. DA, P., KM, E., and KE, Y. (2016). Frailty in HIV: Epidemiology, Biology, Measurement, Interventions, and Research Needs. Curr. HIV AIDS Rep. *13*, 340–348. https://doi.org/10.1007/S11904-016-0334-8.
11. Dogo-Isonagie, C., Lam, S., Gustchina, E., Acharya, P., Yang, Y., Shahzad-ul-Hussan, S., Clore, G.M., Kwong, P.D., and Bewley, C.A. (2012). Peptides from Second Extracellular Loop of C-C Chemokine Receptor Type 5 (CCR5) Inhibit Diverse Strains of HIV-1. J. Biol. Chem. *287*, 15076–15086. https://doi.org/10.1074/JBC.M111.332361.
12. Arrildt, K.T., Joseph, S.B., and Swanstrom, R. (2012). The HIV-1 Env protein: A coat of many colors. Curr. HIV/AIDS Rep. *9*, 52–63. https://doi.org/10.1007/s11904-011-0107-3.
13. Lines, J.A., Yu, Z., Dedkova, L.M., and Chen, S. (2014). Design and expression of a short peptide as an HIV detection probe. Biochem. Biophys. Res. Commun. *443*, 308–312. https://doi.org/10.1016/J.BBRC.2013.11.095.
14. Ko, E., Tran, V.K., Geng, Y., Kim, M.K., Jin, G.H., Son, S.E., Hur, W., and Seong, G.H. (2018). Determination of glycated albumin using boronic acid-derived agarose beads on paper-based devices. Biomicrofluidics *12*, 014111. https://doi.org/10.1063/1.5021395.
15. Wang, F., Yang, C., Duan, M., Tang, Y., and Zhu, J. (2015). TiO2 nanoparticle modified organ-like Ti3C2 MXene nanocomposite encapsulating hemoglobin for a mediator-free biosensor with excellent performances. Biosens. Bioelectron. *74*, 1022–1028. https://doi.org/10.1016/J.BIOS.2015.08.004.
16. Shiying Zhou, P., Sun, H., and Wang, X. (2022). Facile Synthesis of Paper-Derived Porous Activated Carbon and the Electrochemical

Determination of Hydrogen Peroxide You May Also like Fe-Hemin-Metal Organic Frameworks/Three-Dimensional Graphene Composites with Efficient Peroxidase-like Bioactivity for Real-Time Electrochemical Detection of Extracellular Hydrogen. https://doi.org/10.1149/1945-7111/ac6ae8.

17. Chia, H.L., Mayorga-Martinez, C.C., Antonatos, N., Sofer, Z., Gonzalez-Julian, J.J., Webster, R.D., and Pumera, M. (2020). MXene Titanium Carbide-based Biosensor: Strong Dependence of Exfoliation Method on Performance. Anal. Chem. *92*, 2452–2459. https://doi.org/10.1021/ACS.ANALCHEM.9B03634/ASSET/IMAGES/LARGE/AC9B03634_0005.JPEG.
18. Sinha, A., Dhanjai, Mugo, S.M., Chen, J., and Lokesh, K.S. (2020). MXene-based sensors and biosensors: next-generation detection platforms. Handbook of Nanomaterials in Analytical Chemistry: Modern Trends in Analysis, 361–372. https://doi.org/10.1016/B978-0-12-816699-4.00014-1.
19. Zou, G., Zhang, Z., Guo, J., Liu, B., Zhang, Q., Fernandez, C., and Peng, Q. (2016). Synthesis of MXene/Ag Composites for Extraordinary Long Cycle Lifetime Lithium Storage at High Rates. ACS Appl. Mater. Interfaces *8*, 22280–22286. https://doi.org/10.1021/acsami.6b08089.
20. Paul, S., Chakraborty, B.B., Anwar, S., Paul, S.B., and Choudhury, S. (2020). Self-assembly of silver nanoparticles through functionalization with coumarin-thiazole fused-ring thiol. Heliyon *6*, e03674. https://doi.org/10.1016/J.HELIYON.2020.E03674.
21. Li, H., and Du, Z. (2019). Preparation of a Highly Sensitive and Stretchable Strain Sensor of MXene/Silver Nanocomposite-Based Yarn and Wearable Applications. ACS Appl. Mater. Interfaces *11*, 45930–45938. https://doi.org/10.1021/acsami.9b19242.
22. Lin, X., Li, Z., Qiu, J., Wang, Q., Wang, J., Zhang, H., and Chen, T. (2021). Fascinating MXene nanomaterials: emerging opportunities in the biomedical field. Biomater. Sci. *9*, 5437–5471.
23. Rychert, J., Strick, D., Bazner, S., Robinson, J., and Rosenberg, E. Detection of HIV Gp120 in Plasma during Early HIV Infection Is Associated with Increased Proinflammatory and Immunoregulatory Cytokines. 10.1089/aid.2009.0290.
24. Shin, M., Yoon, J., Yi, C., Lee, T., and Choi, J.W. (2019). Flexible HIV-1 Biosensor Based on the Au/MoS2 Nanoparticles/Au Nanolayer on the PET Substrate. Nanomaterials *9*, 1076. https://doi.org/10.3390/NANO9081076.
25. Ma, Y., Liu, C., Wang, M., and Wang, L.S. (2019). Sensitive electrochemical detection of gp120 based on the combination of NBD-556 and gp120. Talanta *196*, 486–492. https://doi.org/10.1016/J.TALANTA.2018.12.062.
26. Lee, J.H., Oh, B.K., and Choi, J.W. (2013). Electrochemical sensor based on direct electron transfer of HIV-1 Virus at Au nanoparticle modified ITO electrode. Biosens. Bioelectron. *49*, 531–535. https://doi.org/10.1016/J.BIOS.2013.06.010.
27. Uygun, Z.O., and Ertuğrul Uygun, H.D. (2014). A short footnote: Circuit design for faradaic impedimetric sensors and biosensors. Sensor. Actuator. B Chem. *202*, 448–453. https://doi.org/10.1016/J.SNB.2014.05.029.
28. Shen, J., Chen, G., Yang, Z., Wu, Y., Ma, C., Li, L., Yang, T., Gu, J., Gao, H., and Zhu, C. (2023). Boric acid-functionalized silver nanoparticles as SERS substrate for sensitive and rapid detection of fructose in artificial urine. Spectrochim. Acta Mol. Biomol. Spectrosc. *288*, 122179. https://doi.org/10.1016/J.SAA.2022.122179.
29. Celigoy, J., Ramirez, B., Tao, L., Rong, L., Yan, L., Feng, Y.R., Quinnan, G.V., Broder, C.C., and Caffrey, M. (2011). Probing the HIV gp120 envelope glycoprotein conformation by NMR. J. Biol. Chem. *286*, 23975–23981. https://doi.org/10.1074/jbc.M111.251025.
30. Ferrer, M., and Harrison, S.C. (1999). Peptide Ligands to Human Immunodeficiency Virus Type 1 gp120 Identified from Phage Display Libraries. J. Virol. *73*, 5795–5802.
31. Ertuğrul Uygun, H.D. Impedimetric CRISPR-dCas9 Based Biosensor System for Sickle Cell Anemia Mutation. https://doi.org/10.18596/jotcsa.

STAR★METHODS

KEY RESOURCES TABLE

REAGENT or RESOURCE	SOURCE	IDENTIFIER
Chemicals, electrodes, peptides and proteins		
HIV-1 gp120 ELISA Kit	Novus Biologicals	Colorimetric-NBP2-80343
HIV-1 gp120 protein recombinant	Merck	SAE0071-100UG
Peptides (Custom)	Merck	Custom Peptides
Carbon electrodes	Metrohm Dropsens	DRP-110
Potassium ferricyanide(III)	Merck	702587
Potassium hexacyanoferrate(II) trihydrate	Merck	P9387
Potassium phosphate monobasic	Merck	529568
MPTES	Merck	175617
Hydrogen fluoride	Merck	8.18068
Ti_3AlC_2	Merck	910775
$AgNO_3$	Merck	209139
DMSO	Merck	D276855
KCl	Merck	P9333
Gold(III) chloride trihydrate	Merck	520918-1G
Biological samples		
Healthy human serum	Healthy subjects pool (10)	N/A
Software and devices		
PSTrace 5.9	PalmSens	https://www.palmsens.com/software/ps-trace/
Origin Pro. 2023	Origin Lab	Learning Edition (originlab.com)

RESOURCE AVAILABILITY

Lead contact

Further information and requests for resources and reagents should be directed to and will be fulfilled by the lead contact, Savas Tasoglu (stasoglu@ku.edu.tr).

Materials availability

This study did not generate new unique reagents.

Data and code availability

- All data reported in this paper will be shared by the lead contact upon request.
- This paper does not report original code.
- Any additional information required to reanalyze the data reported in this paper is available from the lead contact upon request.

EXPERIMENTAL MODEL AND STUDY PARTICIPANT DETAILS

Human samples were collected in the Research Hospital of Kafkas University with permission of Kafkas University, Faculty of Medicine Ethical Committee (28.04.2021; 64-2021/05). Healthy human samples were collected in anticoagulant tubes (2cc) and centrifuged at 2000 rpm. Total 20 mL serum samples were divided into aliquots of 100 μL. Collected samples were stored at -80°C until use.

METHOD DETAILS

Chemicals and reagents

HIV-1 gp120 ELISA Kit (Colorimetric-NBP2-80343) obtained from Novus Biologicals, LLC USA. HIV-1 gp120 protein recombinant, expressed in HEK 293 cells, was obtained from Merck (USA). gp120 protein binding peptides were selected as the synthetic peptide sequence

(RINNIPWSEAMM-$(CH_2)_6$-SH; IC50: 1.1 μM) Merck (USA). Carbon electrodes (DRP-110) were obtained from Metrohm Dropsens AG (Switzerland). Working and auxiliary electrodes were made of carbon, while the reference electrode was composed of silver/silver chloride. All electrochemical detections were carried out by PalmSens EmStat4S Potentiostate (Netherlands) with PSTrace 5.9 interface.

Electrochemical modifications and methods

Cyclic voltammetry (CV) and Electrochemical Impedance Spectroscopy (EIS) experiments were carried out using a redox probe in 5 mM $Fe(CN)_6^{3-/4-}$ and 100 mM KCl pH 7, phosphate buffer (50 mM). EIS data were calculated using the circuit element for a good fit of the obtained curve.[27] Carbon electrodes were modified by a gold layer, 3-mercaptopropyltrimethoxysilane (MPTES) and MXene-AgNPs to immobilize SH terminated antimicrobial peptides.

MXene-silver nanoparticle synthesis

MXene production was performed based on a previously developed protocol.[21] Hydrogen fluoride (HF) was used as the etching agent. Firstly, Ti_3AlC_2 (1.5 g) was added to HF (40%, 45 mL) and stirred for 24 h in room temperature to form MAX phase. The mixture was centrifuged and then washed 10 times under nitrogen to prevent oxidation (3500 rpm), increase pH, and remove impurities. The black materials obtained were dissolved in DMSO and mixed for 24 h to delaminate. Centrifugation-washing cycle was performed again to avoid impurities. The $Ti_3C_2T_X$ obtained was dried under vacuum. Silver nanoparticles were synthesized on the $Ti_3C_2T_X$ as the reducing agent. To obtain more binding sites for the peptides, $AgNO_3$ (30 mM) was dropped on 1 mg / 60 mL previously sonicated $Ti_3C_2T_X$ (1:3, v/v). The mixture was sonicated for 20 min and dried under vacuum. The nanocomposites were characterized on the electrode surface by SEM with EDX.

Biosensor modification and optimizations

Carbon electrodes (CE) were washed with pure water and dipped in gold solution (30 mM). -0.2 V was applied for 600 s to deposit gold (AuE). To form hydroxyl groups, the electrode was dipped in MPTES (1 mM) and ethanol and incubated for two hours at room temperature (Au-MPTES). Then MXene-AgNPs (1 mg mL^{-1}) was dissolved (water: ethanol, v/v, 1:9). The MXene-AgNPs solution was dropped on MPTES modified gold electrode and incubated under humidified environment for 2 h (AuE-MPTES-MXene-AgNPs). The peptides (5 mg mL^{-1}) were immobilized on the surface that was modified with SH to AgNPs bonding on MXene.[28] Other electrodes with MPTES modifications were prepared using only MXene and only AgNPs to evaluate the difference in sensitivity. This peptide sequence was selected by considering the target gp120 protein (peptide 12p1 sequence: RINNIPWSEAMM) from the peptide database (dbaasp.org) with the lowest IC50, which provided high affinity and selectivity. The peptide has specific binding properties appropriate for the target molecule,[29,30] which acts as an antagonist for the gp120 protein. NMW studies have demonstrated that 12p1 has overlapping binding sites on gp120. This was supported by the observation that 12p1 could compete effectively with 12p1, which displayed phage binding to gp120, suggesting overlapping or allosterically related binding sites. Peptide 12p1 inhibits the interaction between gp120 and both four-domain soluble CD4 (4dCD4) and monoclonal antibody (MAb) 17b. These findings showed that specific binding sites (those not interacting the specific binding site of gp120 and the peptide) provided a unique biorecognition receptor. Therefore, we modified our biosensor with those peptides. These modification steps were electrochemically investigated by CV and EIS. SEM data included the EDX elemental analysis to verify the biosensor surface and MXene-AgNPs composite. CV parameters were set according to the redox probe as -0.2 V to 0.5 V with 100 mV s^{-1} scan rate. EIS parameters were also set between 10000 Hz to 0.05 Hz by applying 180 mV DC and 10 mV AC.[31] Chronoimpedimetric detection was carried out by applying 200 mV for 3600 s with 580 Hz frequency that was obtained in the peptide modification step of the Bode plot. Serum samples were spiked randomly between the ELISA test ranges (34.38-2200 pg mL^{-1}, sensitivity 14.47 pg mL^{-1}). After the modification steps were performed, gp120 binding was tested by dipping the biosensor in 100 pg mL^{-1} gp120 standard solution. Taking the buffer as blank, serum samples without gp120 and gp120 standard solutions were tested to obtain biosensor response and matrix effect. After obtaining the biosensor response time, a calibration range was determined and impedance values were used to compare the concentrations. The impedance values of the calibration curve were calculated by the circuit model, which was compatible with impedance spectrum characteristics. This calibration curve experiments were performed five times to obtain reproducibility by comparing the regression coefficients (R^2) of the calibration curves. Subsequently, LOD and LOQ were calculated using the standard deviation of the lowest concentration and the slope of the calibration curves, which also provided repeatability. The biosensor performance was compared with the spiked serum samples using the ELISA test. Performance parameters of the biosensor such as reusability and storage stability were tested for one month at room temperature and +4°C.

QUANTIFICATION AND STATISTICAL ANALYSIS

Not applicable.